J|A|C|S COMMUNICATIONS

Published on Web 09/23/2009

Pearling of Lipid Vesicles Induced by Nanoparticles

Yan Yu and Steve Granick*

Department of Material Science and Enginering, University of Illinois, Urbana, Illinois 61801

Received July 15, 2009; E-mail: sgranick@illinois.edu

One of the challenges, in using phospholipid vesicles to emulate the membranes of living cells, is to create shape transformations. Here we study in single-component vesicles the shape transformation known as pearling. It is known that bacteria without division machinery can proliferate by forming protrusions from the cell, which gradually evolve to a string of round progeny cells.[1] In eukaryotic cells, tubular protrusions transform into periodic chains of "pearls" upon disrupting the actin cytoskeleton.[2] Alternatively, pearling in neuronal axons and blood vessels can be induced by osmotic stress.[3] Seeking a general understanding, we note that these shape changes are remarkably similar to the classical Rayleigh instability in which a cylindrical fluid stream breaks into droplets. Indeed, tubular lipid vesicles can also break up in this way, for example under the stimulus of anchoring amphiphilic polymers into the membrane outer leaflet, which causes local spontaneous curvature,[4] and under the stimulus of tension induced by optical tweezers.[5] One previous study also found this effect in an originally oblate lipid vesicle, induced by amphiphilic polymer insertion,[6] but the resulting pearl structure was not stable and its breaking up was not controllable. Here we show how to stimulate phospholipid vesicles to transform from the usual sphere structure into pearls and pearl necklaces that are stable for hours.

The environmental stimulus presented here consists in allowing nanoparticles to adsorb onto the inner leaflet of giant unilamellar vesicles (GUVs); this contrasts with previous studies in which polymers and proteins formed membrane inclusions. It is effective at sub-nM nanoparticle concentrations, a concentration range orders of magnitude less than the case using other methods. In contrast to shearing used in model protocells,[7] here the nanoparticle concentration spontaneously determines the pearling division. Furthermore, the effect varies systematically with nanoparticle concentration, enabling the final structures to be controlled.

Giant unilamellar vesicles were prepared using the gentle hydration method.[8] Briefly, mixtures of 1,2-dioleoyl-*sn*-glycero-3-phosphocholine (DOPC) and the fluorescent lipid 1,2-dioleoyl-*sn*-glycero-3-phosphoethanolamine-*N*-(lissamine rhodamine B sulfonyl) (DOPE-RhB) (Avanti Lipids) in choloroform/methanol (2/1 by volume) were dried to form a thin lipid film at the bottom of a flask and hydrated with 0.1 M sucrose containing a given amount of aliphatic amine nanoparticles (usual diameter 200 nm, surface charge 40 Å^2/charge group (Invitrogen Inc.)) overnight at 40 °C. The GUVs were mixed with 0.1 M glucose at 1:1 (v/v) and centrifuged at 2000 rad/s for 1 min. The sedimented GUVs were gently rediluted in 0.1 M sucrose solution for fluorescence imaging. By doing so, nearly all of the nanoparticles located outside of GUVs were removed. GUVs were imaged using a home-built epifluorescence microscope. In control experiments, we confirmed that the presence of sucrose was not necessary for pearling; it simply presented an experimental convenience by assisting sedimentation. The GUV handling procedure did not cause the pearling either. The generality of these findings was confirmed using other cationic nanoparticles, 40 and 100 nm in diameter. For all of these particles,

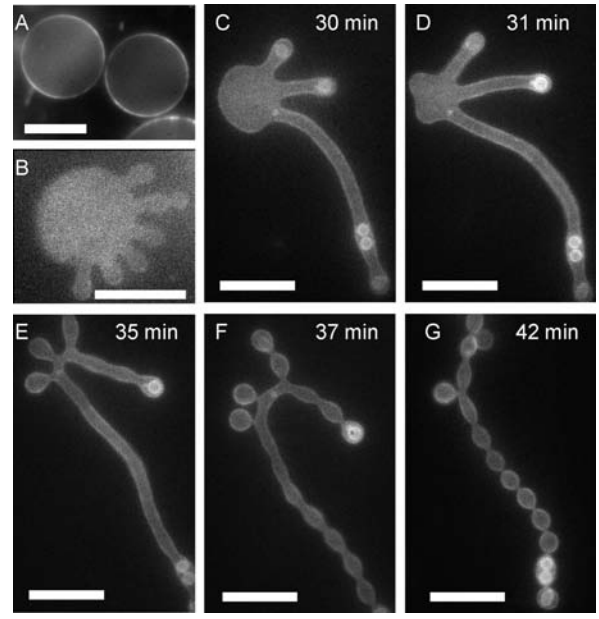

Figure 1. Shape transformation of DOPC giant unilamellar vesicles (GUVs). (A) In the absence of nanoparticles, GUV shape is spherical. (B) In the presence of 0.01 nM cationic nanoparticles (see text), tubular protrusions form. (C−G) The dynamic process illustrated over 12 min as indicated in the panels. Time elapsed after the removal of the nanoparticles located outside of the GUVs. The final state, ellipsoidal pearls of uniform size, strung into a necklace, is stable for hours. Scale bars: 20 μm.

the ion concentration owing to counterions from the nanoparticles was in the range of 3 μM, for which the Debye screening length was ∼150 nm. The shape transformations failed to occur when the screening length was reduced by adding mM concentrations of $CaCl_2$.

The expected spherical shape in the absence of nanoparticles is illustrated in Figure 1A. When 0.01 nM nanoparticles were encapsulated within the GUVs, we observed their shape to fluctuate vigorously until, after 10−20 min, tubular protrusions with a diameter of ∼5 μm began to grow (Figure 1B). Some protrusions were observed to grow and then shrink back into the parental membrane. Figure 1C−G show the dynamic transformation for a different GUV. Two stages are evident: first, protrusion and growth of tubes from the parent sphere; second, its breakup into pearls. The pearls appeared to develop uniformly. It began as a wave along the cylinder, and within 12 min, the long tubular structure transformed into a periodic string of smaller ellipsoidal vesicles connected by narrow necks. In Figure 1, the string is ∼100 μm long and the pearl vesicles have uniform size, ∼4−5 and ∼12 μm along the short and long axes, respectively. This phenomenon was general, but vesicles on different strings were observed to vary in size, independent of string length, perhaps owing to the expected slightly different nanoparticle concentration within different parent GUVs. The pearl-necklace geometry is stable for the same period

10.1021/ja905900h CCC: $40.75

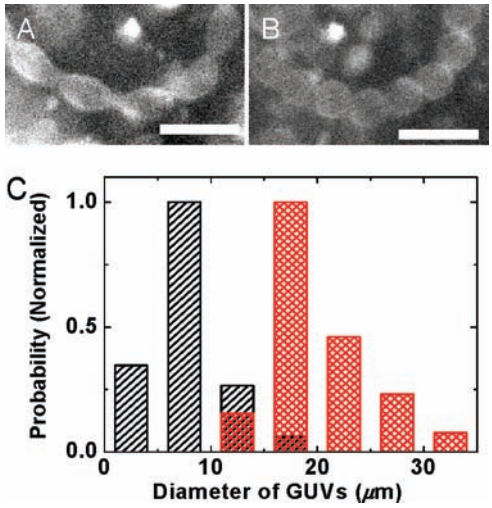

Figure 2. Pearling at higher nanoparticle concentration. The initial stage (A) is followed by transformation of ellipsoids into spheres (B). In panel C, the histogram of vesicle size is compared for no nanoparticles (red) and 10 nM (black), obtained from 50 and 100 disconnected GUVs, respectively. Scale bars: 20 μm.

(several hours) as the lifetime of the parent GUVs. Volume decreases during this shape transformation, but within experimental uncertainty, we estimate the area to be constant.

At a higher (1 nM) nanoparticle concentration, the pearl necklace formed in the early stages and then transformed into discrete spherical pearls of uniform size, which nonetheless remained linked as a chain. The average pearl size was not affected. When the nanoparticle concentration was even higher (10 nM), the chains dissociated rapidly into separated vesicles. Figure 2A contrasts the early stage of this process with the late stage (Figure 2B), observed 20 min later. The size distribution of 100 disconnected GUVs for encapsulated nanoparticle concentrations of 10 nM and 50 GUVs with no nanoparticles is plotted in Figure 2C. It is evident that the higher nanoparticle concentration resulted in smaller vesicles, a factor of 2 smaller. Control experiments showed that shape transformation occurred only in the case of excess nanoparticles encapsulated within the parent GUVs. No shape changes occurred when the nanoparticle adsorbed only to the GUV exterior or when this concentration was the same outside and inside. Indeed, in experiments where shape was induced to change in the usual manner and then nanoparticles were added back into the external medium, we observed that tubules shrank back, reverting to their original spherical shapes. Anionic nanoparticles induced no shape change under any circumstance. Unlike the traditional approach in which the environmental stimulus is from membrane proteins[9] and polymer anchors[4] embedded within lipid tails, these cationic nanoparticles did not appear to be embedded in the membrane and were found to be *mobile* in the adsorbed state. Figure 3 shows individual trajectories of three nanoparticles in a parent GUV, illustrating their diffusion mainly along the membrane rim. Similar findings were obtained for nanoparticles located within tubule protrusions. Our intuitive expectation that nanoparticles would accumulate at regions with a specific curvature of pearls could not be verified within the experimental uncertainty, implying little net accumulation.

It is not the purpose of this study to place these novel observations in the context of the vast theoretical literature on pearling,[10] as the correspondence between the present complex system and the parameters in those theories is unclear. Many possible mechanisms have been proposed.[10] The physical origin here is probably that adsorption of cationic nanoparticles, which increases the headgroup area of zwitterionic lipids,[11] causes a mismatch of surface area between the outer and inner leaflets of the bilayer. The mismatch results in a spontaneous curvature and is enhanced by electrostatic repulsion between the charged nanoparticles, tending to stiffen the membrane and leading to wrinkling and consequently the observed global shape change. But no quantitative explanation is proposed at this time. The main point is that the capacity to control by tuned nanoparticle adsorption the formation and division of pearling in originally spherical lipid vesicles provides a facile strategy to reproduce cellular shape transformations *in vitro*, simply owing to the asymmetric distribution of excess nanoparticle charge inside a GUV.

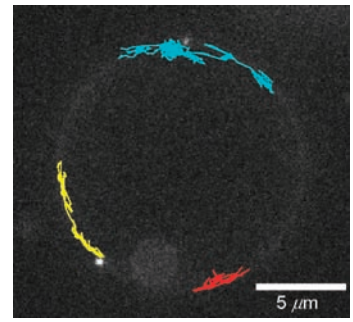

Figure 3. Trajectories of three fluorescent-labeled nanoparticles, indicated in different colors, are illustrated for 0.01 nM concentration, of which 2% were fluorescently labeled. Each time step is 50 ms, and the total lengths range from 5 to 15 s.

Acknowledgment. We thank I. Szleifer and J. Douglas for discussions. This work was supported by the U.S. Department of Energy, Division of Materials Science, under Award No. DEFG02-02ER46019.

References

(1) Leaver, M.; Domínguez-Cuevas, P.; Coxhead, J. M.; Daniel, R. A.; Errington, J. *Nature* **2009**, *457*, 849.
(2) Bar-Ziv, R.; Tlusty, T.; Moses, E.; Safran, S. A.; Bershadsky, A. *Proc. Natl. Acad. Sci. U.S.A.* **1999**, *96*, 10140.
(3) Pullarkat, P. A.; Dommersnes, P.; Fernández, P.; Joanny, J.-F.; Ott, A. *Phys. Rev. Lett.* **2006**, *96*, 048104.
(4) Tsafrir, I.; Sagi, D.; Arzi, T.; Guedeau-Boudeville, M.-A.; Frette, V.; Kandel, D.; Stavans, J. *Phys. Rev. Lett.* **2001**, *86*, 1138.
(5) Bar-Ziv, R.; Moses, E.; Nelson, P. *Biophys. J.* **1998**, *75*, 294.
(6) Tsafrir, I.; Caspi, Y.; Guedeau-Boudeville, M.-A.; Arzi, T.; Stavans, J. *Phys. Rev. Lett.* **2003**, *91*, 138102.
(7) Zhu, T. F.; Szostak, J. W. *J. Am. Chem. Soc.* **2009**, *131*, 5705.
(8) Akashi, K.; Miyata, H.; Itoh, H.; Kinosita, K. *Biophys. J.* **1996**, *71*, 3242.
(9) Sens, P.; Ludger, J.; Bassereau, P. *Curr. Opin. Cell Biol.* **2008**, *20*, 476.
(10) (a) Lipowsky, R.; Döbereiner, H. G. *Europhys. Lett.* **1998**, *43*, 219. (b) Hagedorn, J. G.; Matys, N. S.; Douglas, J. F. *Phys. Rev. E* **2004**, *69*, 056312. (c) Campelo, F.; Hernandez-Machado, A. *Phys. Rev. Lett.* **2007**, *99*, 088101. (d) Nelson, P.; Powers, T.; Seifert, U. *Phys. Rev. Lett.* **2007**, *74*, 3384. (e) Markvoort, A. J.; van Santen, R. A.; Hilbers, P. A. J. *J. Phys. Chem. B* **2006**, *110*, 22780. (f) Reynwar, B. J.; Illya, G.; Harmadaris, V. A.; Müller, M. M.; Kremer, K.; Deserno, M. *Nature* **2007**, *447*, 461. (g) Campelo, F.; Allain, J.-M.; Amar, M. B. *Europhys. Lett.* **2007**, *77*, 38006.
(11) (a) Yu, Y.; Anthony, S. M.; Zhang, L.; Bae, S. C.; Granick, S. *J. Phys. Chem. C* **2007**, *111*, 2833. (b) Wang, B.; Zhang, L.; Bae, S. C.; Granick, S. *Proc. Natl. Acad. Sci. U.S.A.* **2008**, *105*, 18171.

JA905900H